

**NASA TECHNICAL
MEMORANDUM**

NASA TM X-52443

NASA TM X-52443

GPO PRICE \$ _____

CFSTI PRICE(S) \$ _____

Hard copy (HC) 3.00

Microfiche (MF) .65

ff 653 July 65

FACILITY FORM 602

N 68-31094
(ACCESSION NUMBER) (THRU)

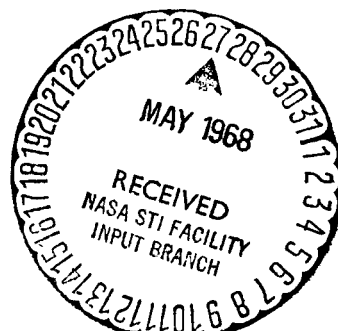
22
(PAGES) (CODE)

✓
(NASA CR OR TMX OR AD NUMBER) (CATEGORY) 03

**CREEPING FLOW SOLUTION OF LEIDENFROST
BOILING WITH A MOVING SURFACE**

by Kenneth J. Baumeister and Glen J. Schoessow
Lewis Research Center
Cleveland, Ohio

TECHNICAL PAPER proposed for presentation at
10th National Heat Transfer Conference sponsored
by the American Institute of Chemical Engineers
and the American Society of Mechanical Engineers
Philadelphia, Pennsylvania, August 11-14, 1968



**CREEPING FLOW SOLUTION OF LEIDENFROST
BOILING WITH A MOVING SURFACE**

by Kenneth J. Baumeister and Glen J. Schoessow

Lewis Research Center
Cleveland, Ohio

TECHNICAL PAPER proposed for presentation at
10th National Heat Transfer Conference
sponsored by the American Institute of Chemical Engineers
and the American Society of Mechanical Engineers
Philadelphia, Pennsylvania, August 11-14, 1968

NATIONAL AERONAUTICS AND SPACE ADMINISTRATION

CREEPING FLOW SOLUTION OF LEIDENFROST

BOILING WITH A MOVING SURFACE

by Kenneth J. Baumeister
Lewis Research Center
National Aeronautics and Space Administration
Cleveland, Ohio

and Glen J. Schoessow
University of Florida
Gainesville, Florida

ABSTRACT

The total vaporization time of water drops in Leidenfrost boiling with supporting plate velocities up to 15 ft/sec has been correlated with a standard deviation of 4.5 percent. The analytical model combines stagnation and Couette flow profiles. In this paper, the vaporization time for a drop film boiling on a moving surface is related to the equivalent vaporization time for a smaller drop placed on a stationary surface.

INTRODUCTION

The liquid metal space power Rankine System is presently being considered as a possible auxiliary power source for space application. In the mist flow regime of its boiler, spiral inserts centrifuge entrained liquid droplets to the heated tube wall to provide droplet free vapor to the turbine. At the wall, the liquid droplet undergoes film boiling which resembles the classic stationary Leidenfrost phenomena, except that in this case a relative velocity exists between the drop and the heated tube wall. The present paper considers the effect of this relative velocity on the vaporization times of the liquid droplets in Leidenfrost film boiling.

If liquid drops are placed upon a sufficiently hot surface, vapor will be generated at the underside of the drop at a rate adequate to support the drop (see Fig. 1(a) and (b)). This phenomenon is usually referred to as stationary Leidenfrost film boiling. Reference 1 considered the Leidenfrost phenomenon on a spinning wheel (see Figs. 1(c), (d), and (2)). It showed that the velocity of the heated wheel surface had a significant effect on the vaporization time of the drop (see Fig. 3).

A model will be developed herein to predict the vaporization time of drops on moving surfaces. This model is an extension of the authors' earlier model for Leidenfrost boiling off of stationary surfaces (ref. 2). Table I lists the principal analytical results of reference 2 in dimensionless form for a flat disk model as pictured beneath the table.

Leidenfrost boiling from stationary surfaces has been under extensive study quite recently (refs. 1 to 10). Reference 10, by Wachters, contains a comprehensive literature summary of some very early, as well as recent, analytical and experimental work in this area. For the present paper; however, Bell's and Hoffman's discussion in references 7 and 8, and Bell's educational monograph, reference 9, contain pertinent discussions of some of the assumptions and limitations of the stationary Leidenfrost model presented in reference 2 upon which the present model is built.

Recently, Poppendiek et al. (ref. 5) have developed a practical correlation for the heat transfer coefficient for helical fog flow in a Rankine boiler using a stationary Leidenfrost model. The present analysis will provide a velocity correction factor which will account for the relative velocity that exists between the drop and the supporting surface.

LIST OF SYMBOLS

A	area of drop
A*	dimensionless area of lower surface (see table I)
B _{1,2}	constants, see table II
C _{1,2,...8}	arbitrary constants
C _p	specific heat at constant pressure
F	dimensionless function defined by equation (3)
F _n	dimensionless function defined by equation (5)
f	radiation factor, $1 / \left[1 + \frac{2h_r}{\bar{h}_s \left(1 + \frac{7}{20} \frac{C_p \Delta T}{\lambda} \right)} \right]^3$
	(reference 1)
g	coefficient of gravity
g _c	gravitational constant (conversion constant between mass and force units)
h _s	heat transfer coefficient on stationary surface
h _T	total heat transfer coefficient

h^*	dimensionless heat transfer coefficient (see table I) (conduction mode only)
h_r	radiative coefficient, $\frac{\epsilon_L \bar{\sigma} (T_w^4 - T_s^4)}{(T_w - T_s)}$
\bar{h}_s	h_s evaluated at $V/2$
K	constant, equal to $1/2(1 - 3\delta^2 C_g/U)$
k	thermal conductivity
L	length, see figure 4
l	average drop thickness
l^*	dimensionless average drop thickness, see table I
n	correction factor
P	static pressure
P_0	reference pressure
P_r	Prandtl number, $\frac{C_p \mu}{k}$
r	radius of drop
T	temperature
T_w	wall temperature
T_s	saturation temperature
ΔT	temperature difference, $T_w - T_s$
t	time
t^*	dimensionless time, see table I
U	velocity of plate relative to drop
U^*	dimensionless velocity defined by equation (4)
u	vapor velocity in x direction
V	volume of drop

V^*	dimensionless volume of drop, see table I
w	vapor velocity in y-direction
X	half side of model, see figure 4
x	distance coordinate
y	distance coordinate
z	distance coordinate
β^2	constant given by equations (A21) and (A22), also $\beta^2 = C_4$
Γ	see bottom table II
δ	vapor gap thickness
ϵ_L	liquid emissivity
λ	latent heat of vaporization
λ^*	modified heat of vaporization, $\lambda^* = \lambda \left(1 + \frac{7C_p \Delta T}{20\lambda} \right)^{-3}$ from reference 6
μ	viscosity
ρ_g	vapor density
ρ_L	liquid density
σ	surface tension
$\bar{\sigma}$	Boltzmann constant
Φ	latent to sensible heat ratio, equation (A27)
ψ	stream function
ψ_s	stationary stream function
ψ_c	Couette flow stream function

METHOD OF ANALYSIS

The experimental measured vaporization time of a discrete liquid drop in Leidenfrost boiling can be estimated by a direct integration of an energy balance on the drop:

$$-\lambda\rho_L \frac{dV}{dt} = h_T(V)A(V) \Delta T \quad (1)$$

where the total heat transfer coefficient, h_T , and the drop area A are dependent on the volume V of liquid that exists at any time t . In equation (1), the total heat-transfer rate to the drop, represented by the right side of equation (1), is set equal to the mass evaporation rate times the latent heat of vaporization. The problem, of course, is to relate h_T and A to the properties of the liquid and vapor, plate temperature, and the environmental conditions surrounding the drop.

The mechanism for energy transfer to the drop is assumed herein (see appendix A) to be conduction across the vapor film (in creeping laminar flow) and radiation to both the top and lower surface. Conduction and diffusive evaporation from the upper surface and sides of the drop were neglected. If the vapor concentration above the drop is low as in metastable boiling (ref. 11), diffusive evaporation can be extremely important, as Bell (ref. 3 and 9) points out and as was verified experimentally by Wachters (ref. 10). However, the temperature differences between the plate and the drop are assumed to be very high in this problem. Also, the conduction under the drop is much greater in this problem because of velocity effects. Thus, the assumption concerning diffusive evaporation will be less restrictive in this problem.

In addition, the shape of the drop as described by the expressions in table I will be assumed independent of velocity. Photographs in reference 1 show that the drop shape depends on velocity. However, for the sake of mathematical simplicity, these deviations will be neglected.

With the latter assumptions, only the heat transfer coefficient becomes velocity dependent. Thus, to determine the vaporization times as a function of plate velocity, the following steps are required

(1) Determine the effect of velocity on the heat transfer coefficient.

(2) Substitute the heat transfer coefficient and the geometric relationships from table I into the energy balance, equation (1), and integrate to find the vaporization time of the drop. The latter step is performed in the next section while the first step, that of determining the heat transfer coefficient, is performed in the appendix.

To simplify the derivation of the heat transfer coefficient, the drop is represented by an equivalent square shape as shown in figure 4. The area of the square is set equal to the circular areas listed on table I. A constant gap thickness is assumed beneath the

drop. No flow is assumed in the z direction; however, later a correction is made for the flow in the z direction (see eq. (A33)). The physical properties are assumed constant and evaluated at the film temperature. Also, the medium surrounding the drop is assumed to be saturated vapor and the vapor pulled beneath the drop by the action of the moving plate is assumed to have the same temperature profiles as that which exists beneath the drop. With these assumptions, the heat transfer coefficient derived in the appendix, equation (A34), is

$$h^* = \frac{h_s^*}{\left[(1 + F^2)^{1/2} - F \right]^{1/2}} \quad (2) - (A34)$$

where F as given in equation (2) as

$$F = (2K - 1)(P_r \phi)^{1/2} U^* \quad (3) - (A26)$$

where K is an integration constant to be evaluated by experiment and the dimensionless velocity U^* given in equation (3) is

$$U^* = \frac{U}{\left[\left(\frac{\rho_L}{\rho_g} - 1 \right) g \frac{V}{X^2} \right]^{1/2}} = \frac{U}{\left[4 \left(\frac{\rho_L}{\rho_g} - 1 \right) g \left(\frac{\sigma g_c}{\rho_c g} \right)^{1/2} \lambda^* \right]^{1/2}} \quad (4) - (A28)$$

Here, h_s^* represents the dimensionless heat transfer coefficient to a stationary drop in Film boiling. The expressions for h_s^* are given in table I. The denominator in equation (2) represents a theoretical correction factor which accounts for the effect of velocity on the heat transfer coefficient. The theoretical F factor contains the velocity dependent terms while U^* represents the characteristic dimensionless velocity.

Empirical Velocity correction

For large velocities, the theoretical heat transfer coefficient is proportional to the half power of the velocity as a combination of equations (3) and (4) will show. This seems to be incorrect, at least for the range of data given in reference 1. Consequently, it was necessary to modify F in an empirical fashion. A power factor n is now introduced into equation (3) to give

$$F_n = (2K - 1)(P_r \phi)^{1/2} U^{*n} \quad (5)$$

This correction factor will be carried into the next section to solve for the vaporization time.

ANALYSIS OF VAPORIZATION TIMES

Equation (1) can be conveniently written in dimensionless form. Expressing h_T , V , A , and t in equation (1) in terms of the dimensionless forms (listed in table I) gives

$$-dV^* = h^*A^* dt^* \quad (6)$$

The total heat transfer coefficient h_{eff}^* has been replaced by the theoretical h^* , equation (2), which considers only the conduction mechanism. The relationship between h_{eff}^* and h^* is

$$h_{\text{eff}}^* = \frac{h^*}{f} \quad (7)$$

where f represents a radiation factor. The factor f is defined in the list of symbols and derived in references (1) and (2). This factor considers radiation to both the top and bottom of the drop. The f factor was absorbed into the definition of t^* .

Equation (6) can now be integrated for the various domains of volume V^* defined in table I. Because of the complexity of equation (2), a closed form solution could not be obtained. However, by evaluating the function F at a reference volume of $V^*/2$ in the volume range of interest, a simple closed form expression for the vaporization time was obtained. The reference volume technique, quite surprisingly, correlated the experimental data better than a number of more complicated integration techniques.

Substituting the value of h^* from equations (2) and (5) along with h_g^* , λ^* and A^* from table I into equation (6) and performing the integration for the various volume domains shown in table I gives the results tabulated in table II.

The equations for the vaporization times, t^* , in table II are of the same functional form as that in table I for the stationary case. In this case, however, V^* is replaced by a velocity-corrected pseudo-volume V^+ given in the last column in table II. For the case when $U = 0$, the dimensionless velocity U^* is zero. Thus, F_n is zero and the pseudo volume V^+ is identical to V^* .

The integration for V^* greater than 0.8 requires that the integration be broken up into two ranges since the forms of equation (6) are different in each volume regime. Consequently, for V^* greater than 0.8, the integration is from V^* to 0.8 and from 0.8 to zero. A similar approach is used for V^* greater than 155.

Breaking up of the integration leads to the constants B_1 and B_2 listed below table II. Of course, a different reference volume is used for each volume range.

SIGNIFICANCE OF PSEUDO VOLUME V^+

When a drop of liquid with dimensionless volume V^* is placed on a stationary plate, the dimensionless vaporization time can be estimated from the formulas given in table I. However, if the plate were given a velocity with respect to the drop, the actual vaporization time would be much smaller than the vaporization time predicted from the stationary equations, as deduced from figure 3.

The general expressions for stationary vaporization time, however, can still be used in the case where a relative velocity exists between the drop and the plate. Equations in table II indicate that a smaller pseudo dimensionless volume V^+ if placed on a stationary surface would evaporate in the same amount of time as a larger real volume V^* which is placed on a moving surface.

COMPARISON OF EXPERIMENT TO THEORY

The experimental data of reference 1 was correlated by optimizing the value of K in equation (3) and n in equation (5) to give the best fit of the data. The integration constant K was 1.3 while the velocity correction parameter n was 0.4. As seen in figure 5, these values correlate the data quite nicely with a standard deviation of only 4.5 percent.

The value of n equal to 0.4 indicates that the heat transfer coefficient is a function of velocity to the 0.2 power. This agrees closely with the experimentally determined values of 0.171 and 0.227 listed in reference 1.

The major advantage of the present semi-theoretical correlation as compared to the purely empirical correlation given in reference 1 is the possibility that the dimensionless groups and constants would be universal and apply to all fluids. Some preliminary data taken at the University of Florida by Charles Wood for Ethanol, Carbon Tetrachloride and Benzene indicate that the present correlation is applicable to a wide range of fluids.

CONCLUSIONS

The velocity effects on the vaporization time can be accounted for by the introduction of a pseudo volume V^+ using the property groups and constants predicted by a relatively simple flow model.

APPENDIX - HEAT TRANSFER COEFFICIENT

The heat transfer coefficients from the plate to the drop are obtained by solving the momentum and energy equations for flow and heat transfer in the vapor gap beneath the drop.

For the assumptions noted in the body of the report (see Method of Analysis Section) the governing differential equations are

Momentum:

$$0 = -g_c \frac{\partial P}{\partial x} + \mu \left(\frac{\partial^2 u}{\partial x^2} + \frac{\partial^2 u}{\partial y^2} \right) \quad (A1)$$

$$0 = -g_c \frac{\partial P}{\partial y} + \mu \left(\frac{\partial^2 w}{\partial x^2} + \frac{\partial^2 w}{\partial y^2} \right) \quad (A2)$$

Continuity:

$$\frac{\partial u}{\partial x} + \frac{\partial w}{\partial y} = 0 \quad (A3)$$

Energy:

$$q = + \frac{k(T_w - T_s)}{\delta} \quad (A4)$$

Boundary Conditions:

$$y = 0 \quad u = U \quad w = 0 \quad T = T_w \quad (A5)$$

$$y = \delta \quad u = 0 \quad w = w(\delta) \quad T = T_s \quad (A6)$$

$$x = +X \quad P = P_0 \quad \text{at } y = \delta \quad (A7)$$

In boundary condition (A5), the drop is fixed and the plate is assumed to move with velocity U , as might be approximated by the experiment depicted in figure 2.

Static Force Constraint:

$$(\rho_L - \rho_g) \frac{g}{g_c} V = \int_{-X}^X (P - P_0) L dx \quad (A8)$$

at $y = \delta$

Interface Energy Balance (Neglecting Radiation):

$$-\rho_g \lambda w(\delta) = \frac{k(T_w - T_s)}{\delta} \quad (A9)$$

The differential energy equation has been replaced by the simple conduction equation (A4); however, a correction for the convection heating of the vapor will be made later using the results of reference 6. Equations (A8) and (A9) are additional and necessary constraints which couple the energy and momentum equations. Equation (A8) requires that the integral of pressure beneath the drop be equal to the drop's weight. Equation (A9) says that latent heat release at the drop surface must be balanced by the heat conduction across the gap. The bulk liquid is assumed to be at the saturation temperature.

Boundary condition (A7) deserves some special comment. Using a uniform gap model to predict the heat transfer coefficient will require that the pressure at the front (-X) and the rear (+X) be different. As will be shown later this pressure difference is extremely small. Because of the complicated flow pattern around the drop (see fig. 2(d)) it is conceptually possible that such a pressure difference could occur, although such a pressure difference can be considered pseudo. A model could be developed in which the pressure is equal at the front and rear by using the slider bearing model (ref. 12, page 98). In this case the gap thickness would be a linear function of position in which the slope could be determined by some added constraint or experiment. However, the uniform gap model was chosen because of its simplicity and because it does lead to a good correlation.

Momentum Equations

The momentum equations are easily solved by use of the stream functions:

$$u = - \frac{\partial \psi}{\partial y} \quad (A10)$$

$$w = + \frac{\partial \psi}{\partial x} \quad (A11)$$

Using these definitions the governing momentum equations can be combined into a single equation with continuity identically satisfied (ref. 12, page 59):

$$\left(\frac{\partial^4}{\partial x^4} + 2 \frac{\partial^4}{\partial x^2 \partial y^2} + \frac{\partial^4}{\partial y^4} \right) \psi = 0 \quad (A12)$$

The problem now is simply to find a stream function which satisfies equation (A12) and the boundary conditions. To find ψ , assume

$$\psi = \psi_s(x,y) + \psi_c(y) \quad (\text{A13})$$

The stream function ψ_s is the stationary stream function which would result if a stationary plate supported the drop, while ψ_c is a stream function representing Couette flow. They are superimposed in order to satisfy the boundary conditions.

Assuming that the variables are separable, gives

$$\psi_s = x(C_1 + C_2y + C_3y^2 + C_4y^3) \quad (\text{A14})$$

while ψ_c can be found by direct integration of equation (A12)

$$\psi_c = C_5 + C_6y + C_7y^2 + C_8y^3 \quad (\text{A15})$$

Combining the two stream functions, equations (A14) and (A15) in equation (A13), determining the velocities from equations (A10) and (A11), and applying the boundary conditions in equations (A5) and (A6) yields

$$u = 3x\beta^2(y\delta - y^2) + U \left[1 - \frac{2Ky}{\delta} - (1 - 2K) \frac{y^2}{\delta^2} \right] \quad (\text{A16})$$

$$w = -\beta^2 \left(\frac{3}{2} \delta y^2 - y^3 \right) \quad (\text{A17})$$

Not all the constants C 's were determined from the boundary conditions. The undetermined constants have been relabeled β^2 and K (see monemclature). The constant β^2 and the gap thickness δ will be determined later by applying equations (A8) and (A9). The constant K will be discussed later in this appendix.

Pressure Distribution

Knowing the velocities under the drop allows us to determine the pressure distribution beneath the drop. Substituting the velocity distribution back into the momentum equations gives

$$\frac{\partial P}{\partial x} = \frac{\mu}{g_c} \left[-6x\beta^2 + \frac{2(2K - 1)U}{\delta^2} \right] \quad (\text{A18})$$

$$\frac{\partial P}{\partial y} = - \frac{\beta^2 \mu (3\delta - 6y)}{g_c} \quad (\text{A19})$$

Integrating the above equations subject to the boundary conditions gives

$$P - P_0 = \frac{3\mu\beta^2}{g_c} \left[(X^2 - x^2) - (\delta y - y^2) \right] - \frac{\mu U(4K - 2)}{g_c \delta^2} (X - x) \quad (\text{A20})$$

Later, K will be taken as 1.3 (reasons to be given later). This will lead to a pressure slightly below atmospheric (approximately 0.001 atmospheres) at the leading edge of the drop.

Coupling Momentum and Energy

Substituting the expression for pressure into the static pressure balance, integrating, and solving for β^2 gives

$$\beta^2 = \frac{(\rho_L - \rho_g)gV}{8\mu X^4} + \frac{U(4K - 2)}{2\delta^2 X} \quad (\text{A21})$$

where L was set equal to $2X$, that is, the drop was assumed square.

The parameter β^2 can also be determined by the interface energy constraints. Evaluating w at $y = \delta$ in equation (A17), substituting this value of w into the interface energy balance, equation (A9), and solving for β^2 gives

$$\beta^2 = \frac{2k}{\lambda \rho_g} \frac{(T_w - T_s)}{\delta^4} \quad (\text{A22})$$

The momentum and energy equations are coupled by equating equations (A21) and (A22) to give after a little rearranging

$$\delta^4 + \frac{8\mu X^3 U(2K - 1)}{(\rho_L - \rho_g)gV} \delta^2 = \frac{16\mu k \Delta T X^4}{(\rho_L - \rho_g)\rho_g V \lambda g} \quad (\text{A23})$$

Solving for the gap thickness gives

$$\delta = \left(\frac{16\mu k \Delta T}{(\rho_L - \rho_g)\rho_g \lambda^*} \frac{X^4}{gV} \right)^{1/4} \left(\sqrt{F^2 + 1} - F \right)^{1/2} \quad (\text{A24})$$

$$F = (2K - 1) U \left[\frac{\mu \rho_g \lambda^*}{(\rho_L - \rho_g)k \Delta T} \frac{X^2}{gV} \right]^{1/2} \quad (\text{A25})$$

or identically after a little manipulation

$$F = (2K - 1)(P_r \Phi)^{1/2} U^* \quad (A26)$$

where P_r is the Prandtl number (see symbols) and

$$\Phi = \frac{\lambda^*}{c_p \Delta T} \quad (A27)$$

$$U^* = \frac{U}{\left[\left(\frac{\rho_L}{\rho_g} - 1 \right) g \frac{V}{X^2} \right]^{1/2}} = \frac{U}{\left[4 \left(\frac{\rho_L}{\rho_g} - 1 \right) g \left(\frac{\sigma g_c}{\rho_L g} \right)^{1/2} l^* \right]^{1/2}} \quad (A28)$$

(see eq. (A31) for right hand expression)

The latent heat, λ , in equations (A24) and (A27) has been replaced by an effective latent heat which is defined in the list of symbols and derived in reference 6. This accounts for convection terms in the energy equation in an empirical manner.

Length, Area, Volume Relations

The length X and the volume V , appear in equations (A24) and (A28). These parameters can be related to the geometrical forms in table I by the following manipulations

$$V = A l = (2X)^2 l \quad (A29)$$

Therefore

$$\frac{V}{X^2} = 4l = 4 \left(\frac{\sigma g_c}{\rho_L g} \right)^{1/2} l^* \quad (A30)$$

which now can be used in equation (A28). Also,

$$\frac{V}{X^4} = \frac{16V}{A^2} = \frac{16V^*}{\left(\frac{\sigma g_c}{\rho_L g} \right)^{1/2} A^{*2}} \quad (A31)$$

Heat Transfer Coefficient

The heat transfer coefficient in dimensionless form for pure conduction across the gap is

$$h^* = \frac{\frac{k}{\delta}}{\left[\frac{k^3(\rho_L - \rho_g)\rho_L^{1/2}\rho_g g^{3/2}\lambda^*}{\mu \Delta T \sigma^{1/2} g_c^{1/2}} \right]^{1/4}} = \frac{\left(\frac{V^*}{A^*}\right)^{1/4}}{\left(\sqrt{F^2 + 1} - F\right)^{1/2}} \quad (A32)$$

where the value of δ from equation (A24) was substituted into the first part of equation (A32) and V and X in equation (A32) were related by equation (A31). The non-dimensionalizing term used in the heat transfer coefficient is the same one listed in table 1 for the stationary drop.

For the case of zero plate velocity, equation (A32) reduces to

$$h^* = \left(\frac{V^*}{A^*}\right)^{1/4} \approx h_S^* \quad (U = 0) \quad (A33)$$

As can be seen in a comparison to the heat transfer coefficient in table I, $(V^*/A^*)^{1/4}$ is within twenty percent of the stationary heat transfer coefficient which was derived for a symmetric circular drop. Thus, the effect of flow in the z direction beneath the drop shown in figure 5 is compensated for empirically by replacing $(V^*/A^*)^{1/4}$ by h_S^* which yields

$$h^* = \frac{h_S^*}{\left[(F^2 + 1)^{1/2} - F\right]^{1/2}} = \frac{h_S^*}{\left[\left(1 + \frac{1}{F^2}\right)^{1/2} - 1\right]^{1/2} F^{1/2}} \quad (A34)$$

This correction, however, is exact in the limit of zero plate velocity. The denominator represents a velocity correction factor to the stationary heat transfer coefficient, h_S^* .

K-Parameter

The value of F can not be determined as yet since it is a function of the unknown parameter K .

As seen from equation (A34), heat transfer coefficient increases for increasing values of K . At $K = 1/2$, however, h^* equals h_S^* and the velocity has no effect on the heat transfer coefficient. Thus, K must be chosen such that $K > 1/2$.

In addition to affecting heat transfer, the value of K directly affects the velocity distribution, as given by the second term in equation (A16). This term is shown graphically in figure 6. Since the moving plate is the cause of the real or pseudo pressure difference across the drop it is reasonable that no back flow occur; thus, $K \leq 1$. Consequently, K appears to be bracketed in the range $1/2 < K \leq 1$.

The value of K was determined experimentally by correlating the data of reference 1. The experimentally determined K was 1.3, as discussed in the body of this report. It is quite remarkable that the optimal value of K came so close to the upper theoretical limit, as shown in figure 6.

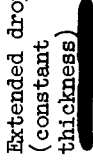
REFERENCES

1. G. J. Schoessow, D. R. Jones, and K. J. Baumeister, "Leidenfrost Film Boiling of Drops on a Moving Surface," Heat Transfer Seattle, Chemical Engineering Progress, Symposium Series, American Institute of Chemical Engineers, 82, volumes 64, 1968.
2. K. J. Baumeister, T. D. Hamill, and G. J. Schoessow, "A Generalized Correlation of Vaporization Times of Drops in Film Boiling on a Flat Plate," Proceedings of the Third International Heat Transfer Conference, Chicago, Illinois, AIChE, vol. 4, 1966, pp. 66-72.
3. B. S. Gottfried, C. J. Lee, and K. J. Bell, "The Leidenfrost Phenomenon: Film Boiling of Small Droplets on a Flat Plate," International Journal of Heat and Mass Transfer, vol. 9, November, 1966, pp. 1167-1187.
4. V. M. Borishansky, "Heat Transfer to a Liquid Freely Flowing Over a Surface Heated to a Temperature Above the Boiling Point. A Collection of Articles," AEC-tr-3405, 1953.
5. H. F. Poppendiek, et al, "Summary Report on High Acceleration Field Heat Transfer for Auxiliary Space Nuclear Power Systems," Geoscience Limited, AEC contract No. AT(04-3)-409, January, 1966.
6. K. J. Baumeister and T. D. Hamill, "Creeping Flow Solution of the Leidenfrost Phenomenon," NASA Technical Note D-3133, 1965.
7. T. W. Hoffman, Discussion of reference 2, Proceedings of the Third International Heat Transfer Conference, Chicago, Illinois, AIChE, vol. 5, 1966, pp. 272, 275.

8. K. J. Bell, Discussion of reference 2, Proceedings of the Third International Heat Transfer Conference, Chicago, Illinois, AIChE, vol. 5, 1966, p. 275.
9. K. J. Bell, "A Generalized Correlation of Vaporization Times of Drops in Film Boiling on a Flat Plate," Educational Monograph HT-2-67, NASA Office of Technology Utilization, contract NSR-37-0020045.
10. L. H. J. Wachters, "Heat Transfer from a Hot Wall to Drops in a Spheroidal State," Doctoral Thesis, Technical University of Delft, The Netherlands, 1965 (Translation under NSF Grant GK607).
11. K. J. Baumeister, R. C. Hendricks, and T. D. Hamill, "Metastable Leidenfrost States," NASA Technical Note D-3226, 1966.
12. H. Schlichting, Boundary Layer Theory, McGraw-Hill Book Company, Inc., New York, N.Y., 1960.

TABLE I. - SUMMARY TABLE FOR STATIONARY DROP RESULTS FROM REFERENCE

[All quantities are in dimensionless form.]

Volume range $V^* = \frac{V}{\left(\frac{\sigma g_c}{\rho_L \beta}\right)^{3/2}}$	Drop shape	Average drop thickness $\lambda^* = \frac{\lambda}{\left(\frac{\sigma g_c}{\rho_L \beta}\right)^{1/2}}$	Area $A^* = \frac{A}{\left(\frac{\sigma g_c}{\rho_L \beta}\right)}$	Heat transfer coefficient $h_g^* = \frac{h}{\left(\frac{k^3 \lambda^* (\rho_L - \rho_g) \rho_L^{1/2} \rho_g^{3/2}}{\Delta T \mu \sigma^{1/2} g_c^{1/2}}\right)^{1/4}}$	Vaporization time* $t^* = \frac{t}{\left(\frac{4^{3/2} \rho_L^{5/2} \mu}{k^3 \lambda^* g^{7/2} (\rho_L - \rho_g) \rho_g \Delta T^3}\right)^{1/4}}$
$V^* \leq 0.8$	Small spheroid 	$\lambda^* = 0.83V^{*1/3}$	$A^* = 1.81V^{*2/3}$	$h_g^* = 1.1V^{*-1/12}$	$t^* = 1.21V^{*5/12}$
$0.8 < V^* \leq 155$	Large drop 	$\lambda^* = 0.8V^{*1/6}$	$A^* = 1.25V^{*5/6}$	$h_g^* = 1.075V^{*-1/6} = 1.2 \left(\frac{V^*}{A^*}\right)^{1/4}$	$t^* = 2.23V^{*1/3} - 0.97$
$V^* > 155$	Extended drop (constant thickness) 	$\lambda^* = 1.85$	$A^* = 0.54V^*$	$h_g^* = 1.64V^{*-1/4} = 1.2 \left(\frac{V^*}{A^*}\right)^{1/4}$	$t^* = 4.52V^{*1/4} - 5.$

*The effect of vapor density on the static force balance of reference 6 has been included here. It was not included in reference 1.

#The V^*/A^* equivalency was not given here because A^* was modified empirically in reference 1 (page 68, equation (23)).



TABLE II. - SUMMARY TABLE FOR MOVING DROP RESULTS

Volume range $V^* = \frac{V}{\left(\frac{\sigma c}{\rho_L g}\right)^{3/2}}$	Drop shape	Vaporization time, $t^* = \frac{t}{\left(\frac{\lambda^4 \rho_L^3 / 2 \sigma^5 / 2.5 / 2 \mu}{k^3 \lambda^* g^{7/2} (\rho_L - \rho_g) \rho_g \Delta T^3}\right)^{1/4}}$	Pseudo velocity dependent volume, V^+
$V^* \lesssim 0.8$	Small spheroid 	$t^* = 1.21 V^{+5/12}$	$V^+ = V^* \Gamma \left(\frac{V^*}{2}\right)^{12/5}$
$0.8 < V^* \lesssim 155$	Large drop 	$t^* = 2.23 V^{+1/3} - 0.97$	$V^+ = V^* \left[\Gamma \left(\frac{V^* + 0.8}{2}\right) + \frac{B_1}{2.23 V^{*1/3}} \right]^3$
$V^* > 155$	Extended drop 	$t^* = 4.52 V^{*1/4} - 5$	$V^+ = V^* \left(\Gamma(V) + \frac{B_2}{4.52 V^{*1/4}} \right)^4$

Constants resulting from integration

$$\Gamma = \left[(1 + F^2)^{1/2} - F \right]^{1/2}$$

$$B_1 = -2.07 \Gamma \left(\frac{V^* + 0.8}{2} \right) + 1.1 \Gamma(0.4) + 0.97$$

$$B_2 = -16 \Gamma(V) + 9.9 \Gamma(77.9) + 1.1 \Gamma(0.4) + 5$$

$\Gamma \left(\frac{V^*}{2} \right)$ means Γ evaluated at V^* equal to $\frac{V^*}{2}$

$\Gamma \left(\frac{V^* + 0.8}{2} \right)$ means Γ evaluated at V^* equal to $\frac{V^* + 0.8}{2}$

$\Gamma(0.4)$ and $\Gamma(77.9)$ means Γ evaluated at V^* equals 0.4 and 77.9 respectively

Stationary Drops

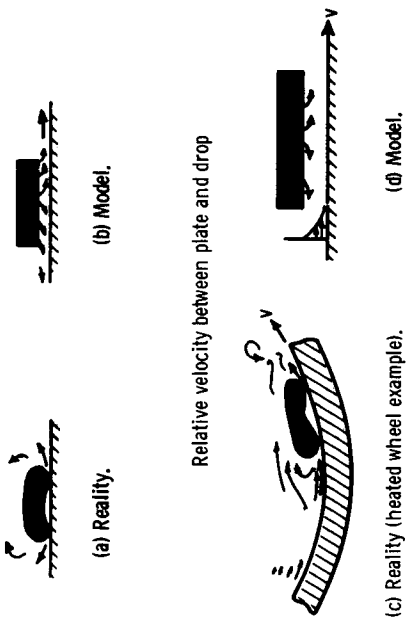


Figure 1. - Sketch of Leidenfrost film boiling with relative velocity between drop and surface (arrows indicate vapor flow).

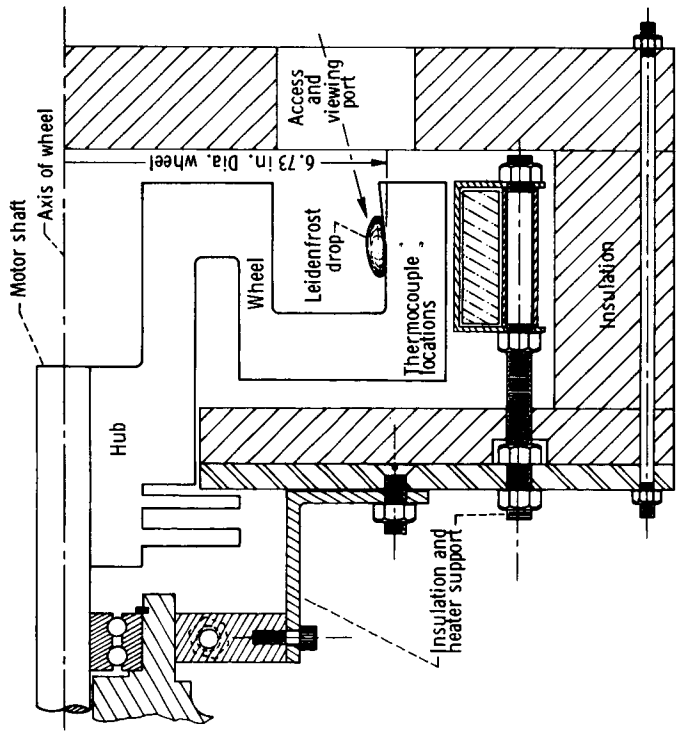


Figure 2. - Cross section of wheel assembly.

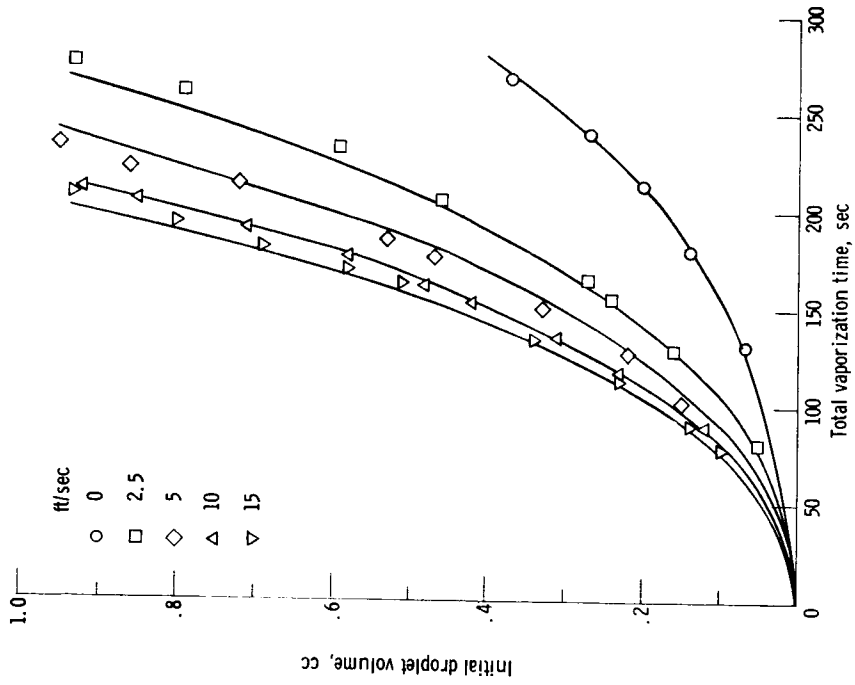


Figure 3. - Droplet vaporization on a flat surface at 304° C.

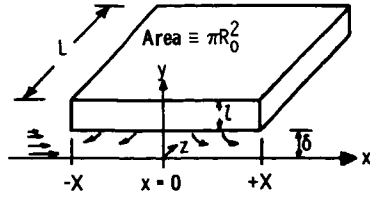


Figure 4. - Flow model.

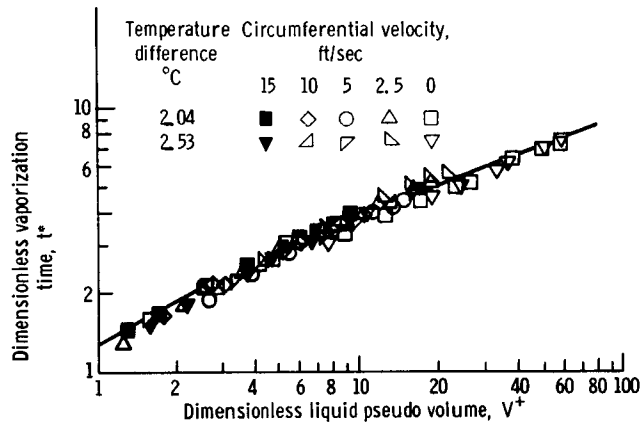


Figure 5. - Total vaporization correlation for $K = 1.3$ and $n = 0.4$.

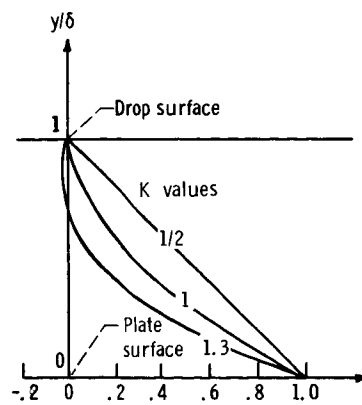


Figure 6. - Couette flow profiles as a function of K (second term in eq. (A16)).